Published in final edited form as:

Nature. 2024 July ; 631(8019): 87–93. doi:10.1038/s41586-024-07474-1.

A deconstruction–reconstruction strategy for pyrimidine diversification

Benjamin J. H. Uhlenbruck[1], **Celena M. Josephitis**[1], **Louis de Lescure**[1], **Robert S. Paton**[1,✉], **Andrew McNally**[1,✉]

[1]Department of Chemistry, Colorado State University, Fort Collins, CO, USA.

Abstract

Structure–activity relationship (SAR) studies are fundamental to drug and agrochemical development, yet only a few synthetic strategies apply to the nitrogen heteroaromatics frequently encountered in small molecule candidates[1–3]. Here we present an alternative approach in which we convert pyrimidine-containing compounds into various other nitrogen heteroaromatics. Transforming pyrimidines into their corresponding *N*-arylpyrimidinium salts enables cleavage into a three-carbon iminoenamine building block, used for various heterocycle-forming reactions. This deconstruction–reconstruction sequence diversifies the initial pyrimidine core and enables access to various heterocycles, such as azoles[4]. In effect, this approach allows heterocycle formation on complex molecules, resulting in analogues that would be challenging to obtain by other methods. We anticipate that this deconstruction–reconstruction strategy will extend to other heterocycle classes.

Modifying the structure of candidate compounds in structure–activity relationship (SAR) studies enables the optimization of their physiochemical properties in drug and agrochemical development[5]. Practitioners commonly select portions of the structure of a candidate to diversify during these studies and altering the periphery of azines, such as pyrimidines, is frequently used because they are pervasive and often form key binding interactions with the biological target[6–9]. Rapid access to analogue compounds is paramount; therefore, chemical reactions that make structural modifications in one or two steps are valuable, particularly during later stages of development involving complex structures[1,2]. Although many individual reactions can transform azines, they typically fall into only two effective

✉**Correspondence and requests for materials** should be addressed to Robert S. Paton or Andrew McNally. Robert.paton@colostate.edu; andy.mcnally@colostate.edu.

Author contributions B.J.H.U. and C.M.J. performed the experimental work. A.M., B.J.H.U. and C.M.J. conceptualized the work. The computational studies were performed by R.S.P. and L.d.L. All authors contributed to the design of the experimental and computational work and to data analysis, discussed the results and commented on the manuscript. A.M. and R.S.P. wrote the manuscript.

Online content

Any methods, additional references, Nature Portfolio reporting summaries, source data, extended data, supplementary information, acknowledgements, peer review information; details of author contributions and competing interests; and statements of data and code availability are available at https://doi.org/10.1038/s41586-024-07474-1.

Competing interests A provisional patent has been filed for this work. The authors declare no other competing interests.

Supplementary information The online version contains supplementary material available at https://doi.org/10.1038/s41586-024-07474-1.

strategies, transforming embedded functional groups and C–H functionalization reactions, which enable rapid diversification for SAR studies[3]. Molecular editing is emerging to produce analogue compounds for SAR studies but is typically associated with transforming one candidate compound to a single derivative[4]. We reasoned that deconstructing complex pyrimidines to a parent synthetic intermediate, with a large set of associated chemical reactions, could expand this strategy. In this way, reconstructing substituted versions of the original pyrimidine and accessing other heterocycles becomes viable through simple cyclization reactions. This approach both diversifies the structure of a candidate and can generate chemical libraries, making it a potentially useful tactic in SAR studies[10].

De novo heterocycle synthesis involves cyclizing smaller chemical fragments into substituted rings, with a classic example being reactions involving 1,3-dicarbonyl compounds to form substituted azines and azoles[5,11]. These processes are commonly used to form building-block pyrimidines, pyrazoles and 1,2-oxazoles. Fragment coupling processes, such as that exploited to create the aminopyrimidine motif in gleevec, also use de novo synthesis; large-member libraries are created this way because of the commercial availability of partners such as amidines and hydrazines (Fig. 1a)[12,13]. Although valuable at earlier points in drug discovery, this strategy is far less suitable for SAR studies on more complex candidate structures. Preserving heterocycle precursors, such as 1,3-dicarbonyls or their derivatives, through several synthetic steps and diversifying at later stages is generally not viable as they tend to react with many classes of organic molecules and reagents. Therefore, developers process building-block heterocycles through rounds of multistep sequences to obtain analogue compounds. Furthermore, key heterocycles are typically extant in advanced candidates, so de novo approaches are ostensibly unsuitable for SAR studies. However, we have devised a strategy that transforms complex pyrimidine-containing structures into iminoenamines, surrogates of 1,3-dicarbonyl compounds, and then leverages de novo heterocycle synthesis to obtain substituted pyrimidine and 1,2-azole analogues. This way, practitioners can envisage a masked, diversifiable three-carbon unit in pyrimidines and strategize for late-stage SAR applications.

We conceived of this alternative approach to exploit de novo heterocycle synthesis based on the unexpected reaction in Fig. 1b. Our laboratory has previously disclosed that pyridines react with Tf_2O and dibenzylamine to form ring-opened Zincke imines, which can be halogenated and recyclized to form 3-halopyridines[14]. When we tested an alternative procedure involving 4-phenylpyrimidine **1a** and aniline as a nucleophile[15], we did not observe ring-opened aza-Zincke imine **2**, but instead obtained *N*-phenylpyrimidinium salt **3a** in high yield[16]. It was then trivial to excise the C2 carbon atom using ethanolic solutions of piperidine and obtained a high yield of iminoenamine **4a** along with minor amounts of a vinamidinium salt as judged by the crude ^{1}H nuclear magnetic resonance (NMR) spectra with an internal standard (Supplementary Fig. 1). Iminoenamines are derivatives of 1,3-dicarbonyl compounds and represent key building blocks for de novo heterocycle synthesis. Figure 1b shows that in situ recyclization using guanidine under basic conditions forms 2-aminopyrimidine **5a** in good yield. Alternatively, adding hydroxylamine and hydrochloric acid to the crude mixture containing **4a** forms 1,2-oxazole **6a** as a mixture of regioisomers. These ‘scaffold hopping’ processes have recently gained attention in the burgeoning area of

molecular editing[17–23]. Sarpong reported that hydrazines react with *N*Tf-pyrimidinium salts and form pyrazoles by means of a ring-opening, ring-closing process[24]. Here, rather than a one-to-one mapping of structures, iminoenamines enable access to several heterocyclic scaffolds[25]. This pilot study successfully demonstrates the principle of using de novo synthesis on existing heterocycles; in the next phase, we aimed to show its generality on various pyrimidine starting materials and cyclization partners.

Figure 2 shows representative examples of pyrimidinium salts formed by means of the ring-opening, ring-closing process, as well as the scope of 2-substituted pyrimidines and 1,2-azoles obtainable after the deconstruction–reconstruction steps. A wide variety of pyrimidines undergo the ring-opening, ring-closing protocol with aniline to form the corresponding pyrimidinium salts and Fig. 2 shows six representative examples (see Supplementary Fig. 4 for 14 more substrates). In general, 4-monosubstituted pyrimidines work well and can include (hetero)aryl groups, alkyl, alkoxy, amido and carbonyl substituents (**3b**–**3d**; Supplementary Fig. 4). In the case of C4 amide-substituted salts, we observed significant aniline triflylation and low yields of the pyrimidinium salt. However, we found that using 2,4,6-trimethylaniline mitigates this unwanted side reaction, resulting in a reasonable yield of salt **3d** (vide infra). The 5-monosubstituted pyrimidines form mixtures of pyrimidinium salts, aza-Zincke imines and aniline-derived iminoenamines (Supplementary Fig. 3). This mixture is less suitable for isolation and characterization at this stage but can be directly taken into the subsequent heterocycle-forming steps (vide infra). On the other hand, 4,5-disubstituted pyrimidines form salts well (**3e** and **3f**), with the chemoselectivity between the pyridine and pyrimidine being notable. We also showed that fused heterocycles, such as *N*Ts-protected deazapurine, are viable substrates (**3g**). However, quinazolines were not successful in the salt-forming process. Other limitations include 4-halopyrimidines, 4-methylpyridimidines and 2-substituted pyrimidines. These cases result in low yields or competitive side reactions, although we are currently investigating how different anilines can alleviate these issues. We provide further information on the limitations of the ring-opening and ring-closing process in Supplementary Fig. 2.

With this robust method for pyrimidinium salt formation in hand, we next examined the scope of the deconstruction–reconstruction process. Cyclizations with urea and thiourea result in pyrimidinone **5b** and thiopyrimidine **5c**, respectively. Constructing 2-substituted pyrimidines with alkyl groups, such as methyl and cyclopropyl, is effective using the corresponding amidines in the cyclization step (**5d** and **5e**). Similarly, using trifluoroacetamidine forms CF_3-substituted pyrimidine **5f** in good yield. The process can also form biheteroaryls, such as **5g**–**5k**, in moderate to good yields. It is important to note that forming the C–heteroatom and C–C bonds in **5b**–**5k** would typically necessitate a (pseudo)halide precursor and require nucleophilic aromatic substitution (S_NAr) or metal-catalysed cross-coupling reactions that could be challenging to implement on complex azines[26,27]. Furthermore, there are only a few pyrimidine C–H functionalization reactions that function on complex substrates[28]. Others reported a 2-selective C–H amination reaction by means of pyrimidine *N*-oxides[29]. As the intermediate is distinct from the *N*Tf-pyridinium salts in this approach, the output scope of these processes is likely to be complementary[29]. Minisci-type processes are ways to construct C–C bonds but they tend to give unselective

mixtures of regioisomers or are biased towards the C4 position. Directed metalation reactions are viable for pyrimidine 2-halogenation in simple substrates[30].

We continued to test this deconstruction–reconstruction approach to effect net C–H functionalization reactions. To that end, we transformed a pyrimidine-containing analogue of pregnenolone into 2-cyclopropylated structure **5l**. Polyazines are compatible and we did not observe any reactions on the pyridine moiety in **5m**, demonstrating chemoselectivity relevant to drug and agrochemical-type molecules[31]. We next examined a series of 5-monosubstituted pyrimidines which resemble drug-like fragments. As described above, these structures form intermediate mixtures at the pyrimidinium salt stage, so we developed a one-pot procedure by exchanging the solvent for ethanol and recyclizing to 2-substituted pyrimidines **5n**–**5p** in reasonable yields. The method also works well to convert pyrimidines into azoles; we formed 1,2-oxazole **6b** from an amido-substituted pyrimidinium salt. The 4-arylated 1,2-oxazole **6c** is another example of deconstructing and reconstructing a 5-substituted pyrimidine. This chemistry also functions on molecules possessing several pyrimidines. Using 4,5-bipyrimidine, we performed a round of pyrimidinium salt formation, cleavage to the iminoenamine and recyclization with *N*-phenylhydrazine to install a pyrazole. Then, a second round culminating instead with hydroxylamine resulted in pyrazole-1,2-oxazole heteroaryl **6d**. The process also functions on 4,5-disubstituted pyrimidines and provides access to disubstituted azoles **6e**–**6g**. See Supplementary Fig. 5 for 20 more examples of 2-substituted pyrimidines and azoles formed through this approach. At present, isoureas and *N*-substituted guanidines are unsuccessful in the recyclization step (Supplementary Fig. 2). We also found that *N*-acyl- and *N*-sulfonylhydrazines result in N–H pyrazoles, indicating cleavage of those groups during recyclization.

At this stage, we turned this deconstruction–reconstruction approach towards modifying biologically active molecules into diverse sets of derivatives in line with strategies used in drug and agrochemical development. First, we converted the fungicide fenarimol (**1b**) into amino, cyclopropyl, and phenyl derivatives **5q**–**5s** in one-pot processes (Fig. 3a). Second, to test a more challenging pyrimidine-containing structure, we selected dabrafenib, a small molecule treatment for melanoma, as a case study[32]. In Fig. 3a, **1c** is a precursor to dabrafenib containing a pyrimidine with a 2-position C–H bond. In a one-pot process that formed the corresponding *N*-arylpyrimidinium salt in situ, we sequentially added piperidine in ethanol to form iminoenamine **4b** followed by guanidine under basic conditions to install the C2–NH_2 group, resulting in the active drug dabrafenib (**5t**). Using the same one-pot protocol, we also successfully obtained cyclopropylated and trifluoromethylated analogues **5u** and **5v** using amidines in the pyrimidine reconstruction stage. We found that scaffold hopping to other heterocycles was viable in this endeavour. In these cases, we obtained higher overall yields from **1c** when we isolated its *N*-arylpyrimidinium salt. Cleavage to iminoenamine **4b** followed by recyclization with hydrazines formed pyrazoles **6h** and, notably, **6i** as a single regioisomer. The same protocol, using hydroxylamine, constructs 1,2-oxazole **6j** as a 16:1 regioisomeric mixture. These six derivatives of **1c** highlight the capacity of the three-carbon iminoenamine intermediate **4b** to serve as a versatile moiety for complex pyrimidine diversification.

Figure 3b shows that it is possible to functionalize the pyrimidine C2 and C5 positions using iminoenamine intermediates. We cleaved pyrimidinium salt **3h** using the standard protocol, then added *N*-chlorosuccinimide and trifluoroacetic acid directly to the reaction mixture to form chloroiminoenamine **4c**. Subjecting the crude mixture to the pyrimidine reconstruction process with cyclopropaneamidine resulted in 2,5-disubstituted product **5w**. The C–Cl bond can be inherently valuable in biologically active molecules and can be used as a functional group for further derivatization at a distinct position of the heterocycle (see Extended Data Fig. 1a for an extra example of pyrimidine C5-chlorination)[33]. Furthermore, this net C–H difunctionalization process is distinct from typical periphery modification reactions which functionalize one position and provides two points to diversify pyrimidines during SAR studies. Further investigations on pyrimidine C5-functionalization using this approach are underway.

Next, we developed processes that transforms pyrimidines into pyridines using a deconstruction–reconstruction approach (Fig. 4). After forming the pyridmidinium salt, a modified version of the C2 cleavage step using pyrrolidine as a nucleophile forms intermediate vinamidinium salts[34]. Previous reports have shown that vinamidinium salts react with ketone-derived enolates and then ammonium salts to form substituted pyridines[35]. We adapted a procedure from Marcoux using the lithium enolate of commercially available acetyltrimethylsilane followed by a mixture of ammonium acetate (NH_4OAc) and acetic acid (AcOH) at 95 °C. As shown in Fig. 4a, we formed pyridines **7a**–**7d** from pyrimidine precursors; we propose that a C6 C–Si bond cleaves after forming the pyridine under the reaction conditions. This modification ensures the formal replacement of a pyrimidine N-atom with a C-atom, which would be a useful manoeuvre in SAR studies[4,36]. Figure 4b shows that choosing the appropriate nucleophile can introduce substituents at the C5 or C2 positions during N to C replacement. For example, using acetyltrimethylsilane as the nucleophile when transforming **3j** results in monosubstituted pyridine **7e** as described above. However, using the dimethylhydrazone derived from butyraldehyde under basic conditions forms disubstituted pyridine **7f**, with a C5 ethyl substituent. In this way, the reconstruction step uses the wealth of aldehydes and the β-substituent resides at the pyridine C5 position. When transforming pyrimidine **1f**, we used methyl ketones in the recyclization step to selectively incorporate C2 substituents in pyridines **7g** and **7h**[35]. Extended Data Fig. 1b shows two more examples of converting pyrimidine **1f** into 2-substituted pyridines and Supplementary Fig. 6 provides a guide for atom incorporation for the transformations in Fig. 4.

In the final part of this project, we studied the mechanism of *N*-arylpyrimidinium salt formation computationally by performing quantum chemical calculations at the ωB97X-D/def2-TZVP//ωB97X-D/6–31+G(d,p) level of theory, with a solvent model based on density (SMD) description of ethyl acetate. Figure 5a shows the computed potential energy surface for the reaction of **1a** with Tf_2O and aniline. The reaction between **1a** and Tf_2O is exergonic (-4.3 kcal mol^{-1}) and proceeds in a single step through **TS-Act** (Gibbs free energy change between the reactants and the transition state, $\Delta G^{\ddagger} = 12.6$ kcal mol^{-1}). Aniline then adds to the resulting *N*Tf-pyrimidinium with nucleophilic attack at C6 ($\Delta G^{\ddagger}$ 15.1 kcal mol^{-1} through **TS-Add-C6**) preferred in place of C2 ($\Delta G^{\ddagger}$ 15.9 kcal mol^{-1} through **TS-Add-C2**),

which corresponds to a kinetic selectivity of 8:1 at −78 °C. These transition structure (TS) energies reflect the electronic Fukui (f^+) indices that indicate greater electrophilicity at C6 versus C2 (0.15 versus 0.10). Although the C6-adduct formed in endergonic by 8.9 kcal mol^{-1}, deprotonation of the ammonium species by collidine occurs in an energetically barrierless process to produce a stable intermediate, **Int-I** (Gibbs free energy change, ΔG = −20.7 kcal mol^{-1}) and indicates that the base drives this process forward.

Next, **Int-I** undergoes facile ring-opening ($\Delta G^{\ddagger}$ 10.7 kcal mol^{-1} through **TS-II**) to form aza-Zincke imine **Int-II** (shown in its most stable *E*, *Z*, *E* configuration), which is thermodynamically favoured by 3.5 kcal mol^{-1}. **Int-II** then tautomerizes and isomerizes to **Int-III** before ring-closing through **TS-IV** ($\Delta G^{\ddagger}$ 18.1 kcal mol^{-1}, relative to **Int-II**) to form dihydropyrimidine derivative **Int-IV** in exergonic fashion (ΔG −4.6 kcal mol^{-1}). Ring closure is the largest barrier along the reaction coordinate, making **TS-IV** rate-limiting. Ejection of a triflamide anion yields a stable ion pair (**Int-V**) and subsequent anion metathesis results in the pyrimidinium triflate **3a** (overall $\Delta G^{\ddagger}$ −34.5 kcal mol^{-1}).

We performed nucleus independent chemical shift calculations (NICS(0)$_{zz}$, B3LYP/6–311+G(d,p) level of theory) at the ring centre of each ring-opening and ring-closing TS, to investigate whether these structures exhibit aromatic shielding patterns characteristic of pericyclic transformations[37]. These calculations gave positive values of 8.6 and 8.0 ppm for **TS-II** and **TS-IV**, respectively. For context, the TS for the 6π-electrocyclization of 1,3,5-hexatriene has a NICS(0)$_{zz}$ value of −29.5 ppm and a barrier of 33.1 kcal mol^{-1} at the same level of theory (Supplementary Fig. 10). Thus, because no aromaticity is found in these TSs, they describe polar processes rather than electrocyclic reactions. These polar reactions have relatively low barriers, may be considered as pseudo-pericyclic and can proceed at much lower temperatures[38,39]. For the minor regioisomer, corresponding to aniline adding at C2, the ring-closing barrier is raised significantly by 8.5 kcal mol^{-1} relative to the major regioisomeric pathway shown. Notably, the ring-closing TS for this minor pathway shows a lower NICS(0)$_{zz}$ value (4.5 ppm), consistent with less polar (and greater pericyclic) character (Supplementary Fig. 9).

Our computation studies indicate that the size and electronic properties of the pyrimidine substituents significantly impact the energy barriers for product formation. We described the effect of 14 different C4-substituents on the barrier for ring closure (**TS-IV**) using a bivariate linear regression model featuring tabulated *A*-values and Hammett σ_p constants (Fig. 5b). In the aza-Zincke imine intermediates (for example, **Int-II**), groups at the 4-position experience destabilizing steric interactions through allylic strain ($A^{1,3}$) relative to the cyclic geometry in **TS-IV**. Ring-closing barriers, therefore, decrease in response to increasing ground state destabilization caused by larger 4-substituents, as exemplified by 4-phenylpyrimidine ($\Delta G^{\ddagger}$ 18.1 kcal mol^{-1}) and 4-methylpyrimidine ($\Delta G^{\ddagger}$ 18.0 kcal mol^{-1}) relative to pyrimidine ($\Delta G^{\ddagger}$ 22.7 kcal mol^{-1}). Electronic effects at the 4-position are also apparent as a result of conjugation with two imine-like carbons; electron-withdrawing groups, such as trifluoromethyl, further destabilize **Int-II**, lowering the cyclization barrier ($\Delta G^{\ddagger}$ 12.7 kcal mol^{-1}). Although a 4-CO_2Me group has a relatively low **TS-IV** barrier ($\Delta G^{\ddagger}$ 16.5 kcal mol^{-1}), we observed moderate yield when transforming **1h** into pyrimidinium salt **3j**. We suspected that electron-deficient pyrimidines may not react efficiently with

Tf_2O in the first step of the salt-forming process. Indeed, we obtained similar barriers for triflyl-transfer from Tf_2O to the pyrimidine **1h** ($\Delta G^{\ddagger}$ 16.6 kcal mol^{-1}) as for aniline ($\Delta G^{\ddagger}$ 15.8 kcal mol^{-1}), suggesting that the unproductive formation of *N*-phenyltriflamide occurs competitively. Supplementary Table 3 suggests that more sterically hindered anilines may mitigate this unwanted pathway.

Extended Data

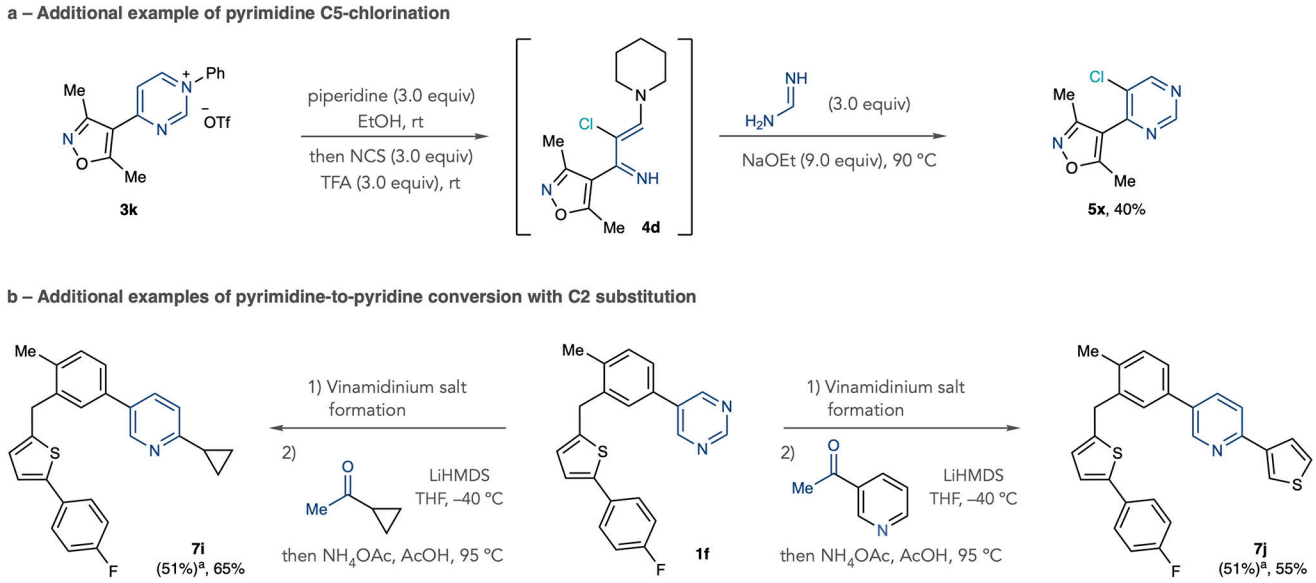

Extended Data Fig. 1 |. Additional examples of pyrimidine functionalization and pyrimidine to pyridine conversion.

a, Additional example of pyrimidine halogenation. **b**, Additional examples of pyrimidine to pyridine conversion using methyl ketones. Isolated yields are shown. Vinamidinium salt formation: Tf_2O (1 equiv), 4-trifluoromethylaniline (1 equiv), collidine (1 equiv), EtOAc, −78 °C to room temperature, then pyrrolidine (6 equiv), EtOH, 60 °C. [a]Isolated yield of vinamidinium salt from pyrimidine.

Supplementary Material

Refer to Web version on PubMed Central for supplementary material.

Acknowledgements

This work was supported by funds from the National Institutes of Health under award no. R01 GM144591 and from the Albert I. Meyers Foundation at Colorado State University. R.S.P. acknowledges support from the NSF (CHE-1955876) and computational resources from the Advanced Cyberinfrastructure Coordination Ecosystem: Services & Support (ACCESS) through allocation TG-CHE180056. This work also used the Alpine high performance computing resource at the University of Colorado Boulder, jointly funded by the University of Colorado Boulder, the University of Colorado Anschutz and Colorado State University.

Data availability

All data are available in the main text or the Supplementary Information.

References

1. Cernak T, Dykstra KD, Tyagarajan S, Vachal P & Krska SW The medicinal chemist's toolbox for late stage functionalization of drug-like molecules. Chem. Soc. Rev 45, 546–576 (2016). [PubMed: 26507237]
2. Zhang L & Ritter T A perspective on late-stage aromatic C–H bond functionalization. J. Am. Chem. Soc 144, 2399–2414 (2022). [PubMed: 35084173]
3. Josephitis CM, Nguyen HMH & McNally A Late-stage C–H functionalization of azines. Chem. Rev 123, 7655–7691 (2023). [PubMed: 37134187]
4. Jurczyk J et al. Single-atom logic for heterocycle editing. Nat. Synth 1, 352–364 (2022). [PubMed: 35935106]
5. Joule JA & Mills K Heterocyclic Chemistry 5th edn (Wiley, 2009).
6. Baumann M & Baxendale IR An overview of the synthetic routes to the best selling drugs containing 6-membered heterocycles. Beilstein J. Org. Chem 9, 2265–2319 (2013). [PubMed: 24204439]
7. Vitaku E, Smith DT & Njardarson JT Analysis of the structural diversity, substitution patterns and frequency of nitrogen heterocycles among U.S. FDA approved pharmaceuticals. J. Med. Chem 57, 10257–10274 (2014). [PubMed: 25255204]
8. Bhutani P et al. U.S. FDA approved drugs from 2015–June 2020: a perspective. J. Med. Chem 64, 2339–2381 (2021). [PubMed: 33617716]
9. Nadar S & Khan T Pyrimidine: an elite heterocyclic leitmotif in drug discovery-synthesis and biological activity. Chem. Biol. Drug Des 100, 818–842 (2022). [PubMed: 34914188]
10. Blakemore DC et al. Organic synthesis provides opportunities to transform drug discovery. Nat. Chem 10, 383–394 (2018). [PubMed: 29568051]
11. Li JJ & Corey EJ Name Reactions in Heterocyclic Chemistry II (Wiley, 2011).
12. Liu YF et al. A facile total synthesis of imatinib base and its analogues. Org. Process Res. Dev 12, 490–495 (2008).
13. CAS SciFindern database search for commercial fragments: amidines 178,649, hydrazines 830,858 (CAS SCIFINDER, accessed November 2023); https://scifinder-n.cas.org.
14. Boyle BT, Levy JN, de Lescure L, Paton RS & McNally A Halogenation of the 3-position of pyridines through Zincke imine intermediates. Science 378, 773–779 (2022). [PubMed: 36395214]
15. Selingo JD et al. A general strategy for *N*-(hetero)arylpiperidine synthesis using Zincke imine intermediates. J. Am. Chem. Soc 146, 936–945 (2023). [PubMed: 38153812]
16. Bartholomew GL et al. ^{14}N to ^{15}N isotopic exchange of nitrogen heteroaromatics through skeletal editing. J. Am. Chem. Soc 146, 2950–2958 (2024). [PubMed: 38286797]
17. Barczynski P & Vanderplas HC Ring transformations in reactions of heterocyclic-compounds with nucleophiles. Conversion of 5-nitropyrimidine into 2-substituted 5-nitropyrimidine and 2-amino-5-nitropyridines by amidines. J. Org. Chem 47, 1077–1080 (1982).
18. Hu Y, Stumpfe D & Bajorath J Recent advances in scaffold hopping. J. Med. Chem 60, 1238–1246 (2017). [PubMed: 28001064]
19. Lamberth C Agrochemical lead optimization by scaffold hopping. Pest Manag. Sci 74, 282–292 (2018). [PubMed: 28991418]
20. Woo J et al. Scaffold hopping by net photochemical carbon deletion of azaarenes. Science 376, 527–532 (2022). [PubMed: 35482853]
21. Dherange BD, Kelly PQ, Liles JP, Sigman MS & Levin MD Carbon atom insertion into pyrroles and indoles promoted by chlorodiazirines. J. Am. Chem. Soc 143, 11337–11344 (2021). [PubMed: 34286965]
22. Reisenbauer JC, Green O, Franchino A, Finkelstein P & Morandi B Late-stage diversification of indole skeletons through nitrogen atom insertion. Science 377, 1104–1109 (2022). [PubMed: 36048958]
23. Patel SC & Burns NZ Conversion of aryl azides to aminopyridines. J. Am. Chem. Soc 144, 17797–17802 (2022). [PubMed: 36135802]

24. Bartholomew GL, Carpaneto F & Sarpong R Skeletal editing of pyrimidines to pyrazoles by formal carbon deletion. J. Am. Chem. Soc 144, 22309–22315 (2022). [PubMed: 36441940]
25. Nishiwaki N, Ogihara T, Takami T, Tamura M & Ariga M New synthetic equivalent of nitromalonaldehyde treatable in organic media. J. Org. Chem 69, 8382–8386 (2004). [PubMed: 15549810]
26. Terrier F Modern Nucleophilic Aromatic Substitution (Wiley-VCH, 2013).
27. Crawley ML & Trost BM Applications of Transition Metal Catalysis in Drug Discovery and Development: An Industrial Perspective (John Wiley & Sons, 2012).
28. Verbitskiy EV, Rusinov GL, Chupakhin ON & Charushin VN Recent advances in direct C–H functionalization of pyrimidines. Synthesis 50, 193–210 (2018).
29. Ham WS, Choi H, Zhang J, Kim D & Chang S C2-selective, functional-group-divergent amination of pyrimidines by enthalpy-controlled nucleophilic functionalization. J. Am. Chem. Soc 144, 2885–2892 (2022). [PubMed: 35138104]
30. Groll K et al. Regioselective metalations of pyrimidines and pyrazines by using frustrated Lewis pairs of BF_3.OEt_2 and hindered magnesium- and zinc-amide bases. Angew. Chem. Int. Ed 52, 6776–6780 (2013).
31. Dolewski RD, Fricke PJ & McNally A Site-selective switching strategies to functionalize polyazines. J. Am. Chem. Soc 140, 8020–8026 (2018). [PubMed: 29792698]
32. Rheault TR et al. Discovery of dabrafenib: a selective inhibitor of Raf kinases with antitumor activity against B-Raf-driven tumors. ACS Med. Chem. Lett 4, 358–362 (2013). [PubMed: 24900673]
33. Chiodi D & Ishihara Y “Magic chloro”: profound effects of the chlorine atom in drug discovery. J. Med. Chem 66, 5305–5331 (2023). [PubMed: 37014977]
34. Mao Y, Tian SX, Zhang W & Xu GY Preparation and application of vinamidinium salts in organic synthesis. Chin. J. Org. Chem 36, 700–710 (2016).
35. Marcoux JF et al. A general preparation of pyridines and pyridones via the annulation of ketones and esters. J. Org. Chem 66, 4194–4199 (2001). [PubMed: 11397153]
36. Pearson TJ et al. Aromatic nitrogen scanning by *ipso*-selective nitrene internalization. Science 381, 1474–1479 (2023). [PubMed: 37769067]
37. Chen Z, Wannere CS, Corminboeuf C, Puchta R & Schleyer P Nucleus-independent chemical shifts (NICS) as an aromaticity criterion. Chem. Rev 105, 3842–3888 (2005). [PubMed: 16218569]
38. Zhou C & Birney DM A density functional theory study clarifying the reactions of conjugated ketenes with formaldimine. A plethora of pericyclic and pseudopericyclic pathways. J. Am. Chem. Soc 124, 5231–5241 (2002). [PubMed: 11982388]
39. Kukier GA, Turlik A, Xue XS & Houk KN Violations. How nature circumvents the Woodward–Hoffmann rules and promotes the forbidden conrotatory 4n + 2 electron electrocyclization of Prinzbach’s vinylogous sesquifulvalene. J. Am. Chem. Soc 143, 21694–21704 (2021). [PubMed: 34911295]

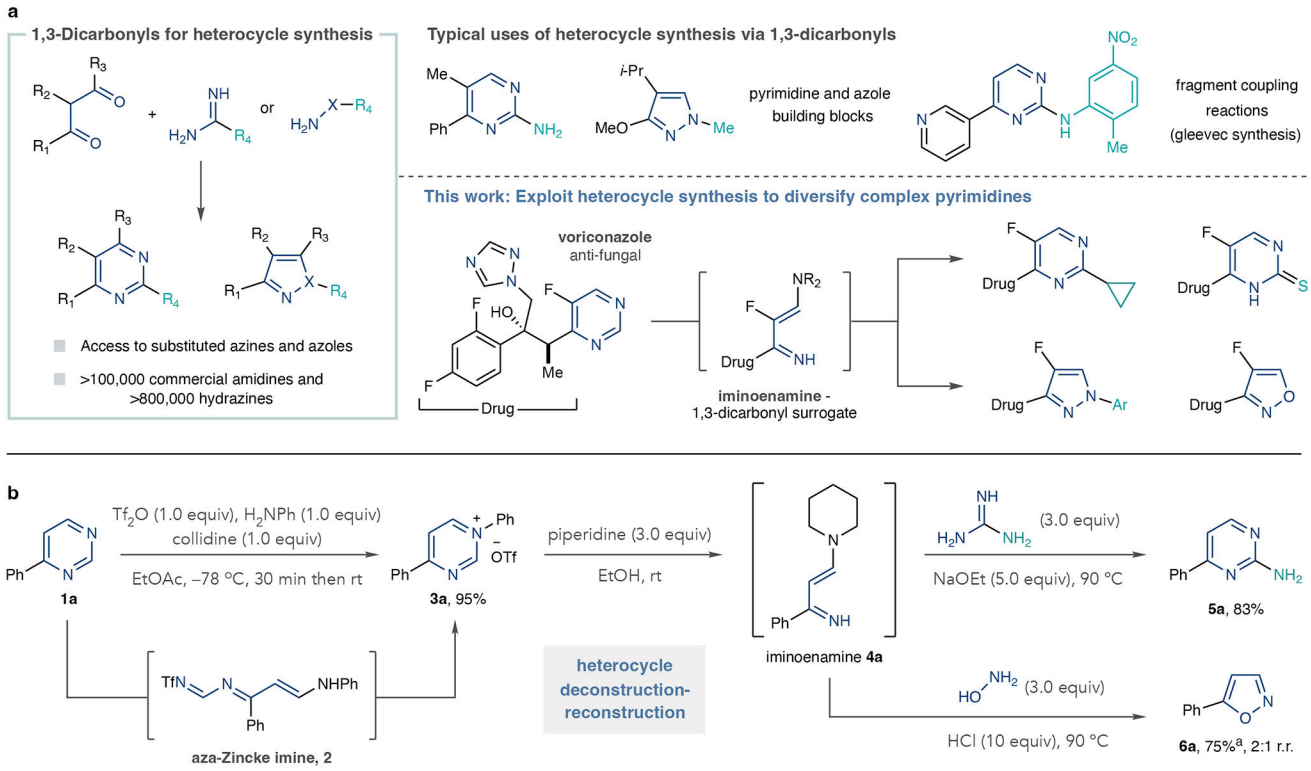

Fig. 1 |. Traditional de novo heterocycle synthesis and a deconstruction– reconstruction approach for heterocycle diversification.

a, Pyrimidine and 1,2-azole synthesis by means of 1,3-dicarbonyls and iminoenamines as potential synthetic intermediates. **b**, Pyrimidine diversification model study showing access to 2-substituted analogues and azoles. Isolated yields are shown. [a]The ^{1}H NMR yield reported due to volatility of **6a**. R denotes a general organic group; X, nitrogen or oxygen atom; Me, methyl; Ph, phenyl; *i*-Pr, iso-propyl; Ar, general aryl group; Tf, trifluoromethylsulfonyl; collidine, 2,4,6-trimethylpyridine; Et, ethyl; Ac, acetate; r.t., room temperature; r.r., regioisomeric ratio.

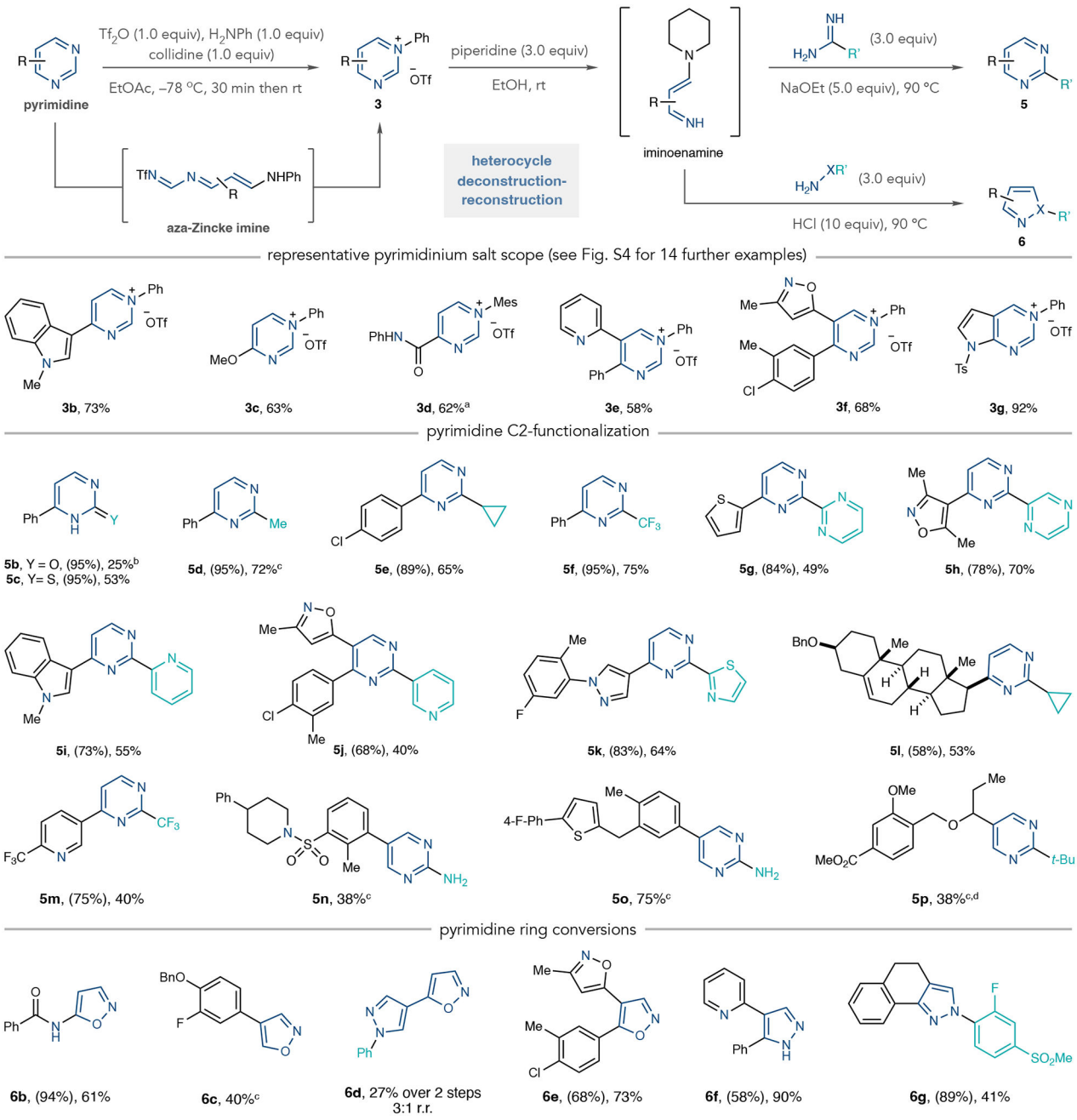

Fig. 2 |. Scope of pyrimidinium salts, 2-substituted pyrimidines and 1,2-azoles.

Isolated yields are shown. Yields in parentheses are for pyrimidinium salts. [a]Instead of aniline, 2,4,6-trimethylaniline was used. [b]Instead of piperidine, 6.0 equivalents of pyrrolidine was used. [c]Isolated as a 17:1 ratio with **1a**. [c]One-pot protocol: 4-nitroaniline used instead of aniline, then the solvent was exchanged for ethanol (EtOH). In the ring-closing step, 10–20 equivalents of amidine or hydroxylamine were used. [d]Sodium methoxide (NaOMe) and methanol (MeOH) used instead of sodium ethoxide (NaOEt) and EtOH. Mes, 2,4,6-trimethylphenyl; Ts, tosyl; Bn, benzyl; *t*-Bu, *tert*-butyl.

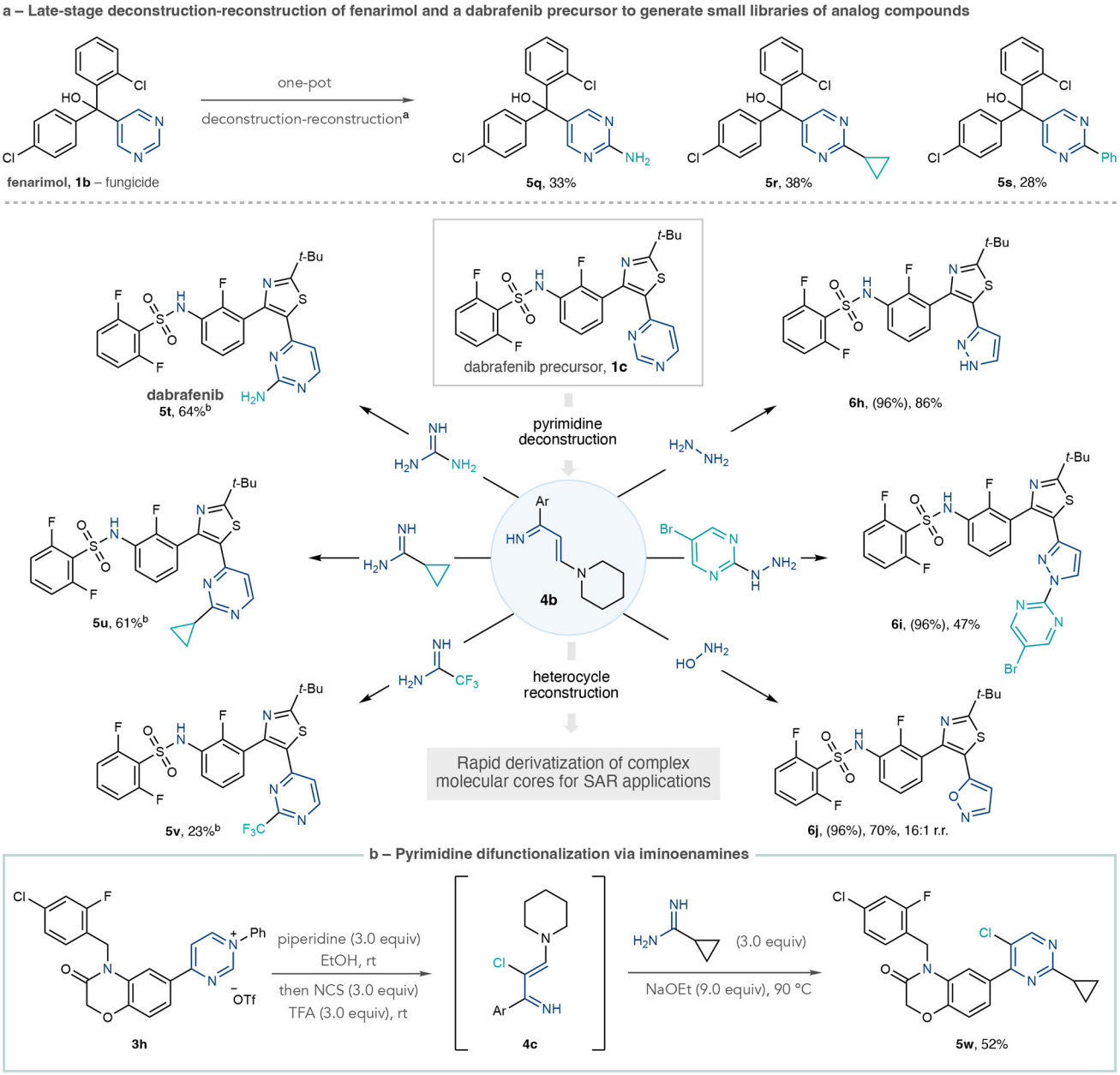

Fig. 3 |. Applications of the pyrimidine diversification strategy to biologically active molecules and further reaction development.

a, Transformations of fenarimol and a dabrafenib precursor. **b**, Pyrimidine halogenation and difunctionalization. Isolated yields are shown. Yields in parentheses are for pyrimidinium salts. [a]One-pot protocol A: Tf_2O (1.0 equiv.), 4-nitroaniline (1.0 equiv.), collidine (1.0 equiv.), EtOAc, −78 °C to room temperature. Solvent exchange to EtOH, then piperidine (3.0 equiv.) at room temperature, then amidine (10–20 equiv.), NaOEt (5.0 equiv.). [b]One-pot protocol B: same as protocol A except using aniline (1.0 equiv.), amidine (3.0 equiv.) at 70 °C and pyrimidinium salt formation conducted in CH_2Cl_2. NCS, *N*-chlorosuccinimide; TFA, trifluoroacetic acid.

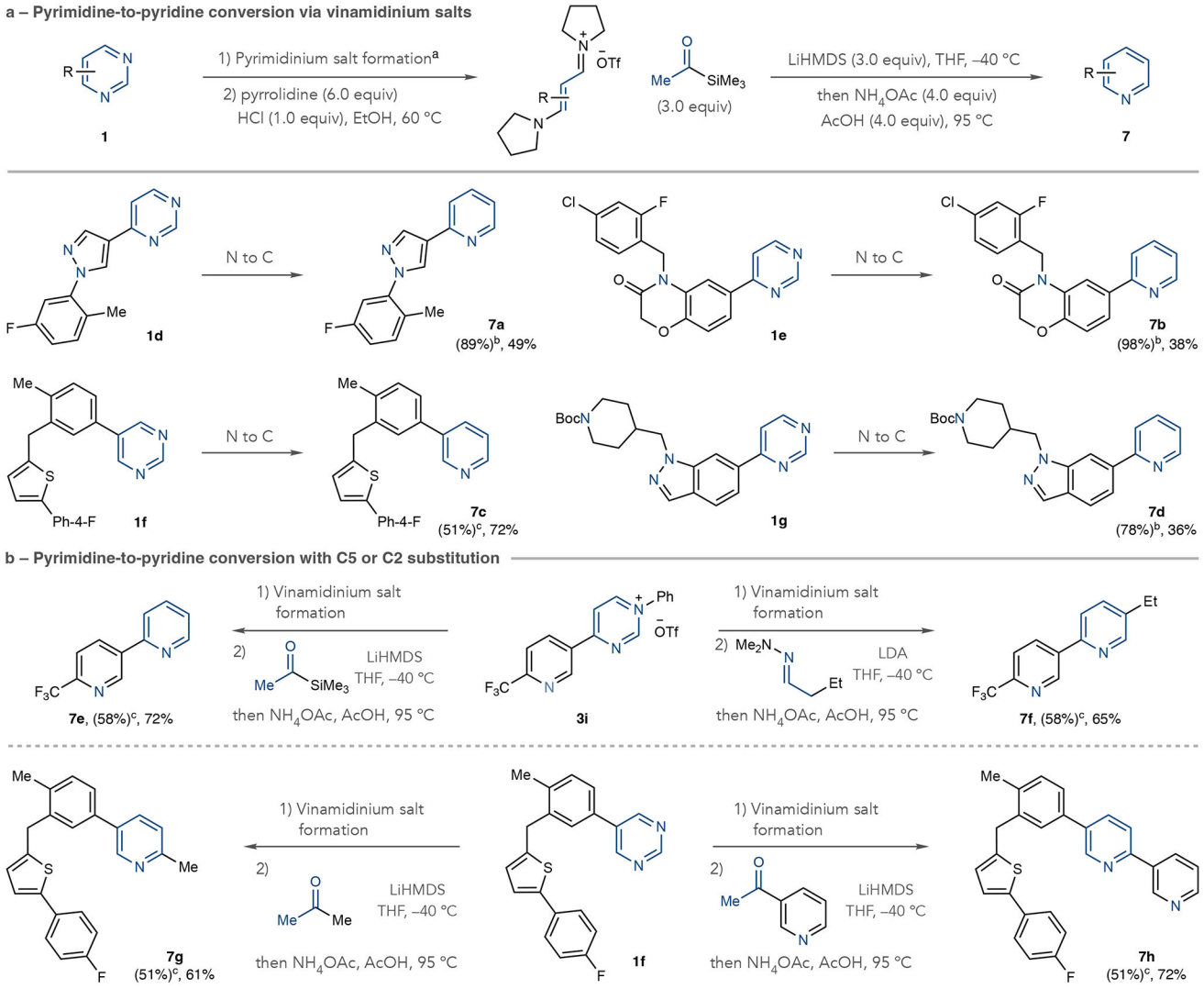

Fig. 4 |. Pyrimidine to pyridine conversions through deconstruction– reconstruction.

a, Transformations using acetyltrimethylsilane as a nucleophile. **b**, Pyridine formation using hydrazones or methyl ketones resulting in C5 or C2 substitution. Isolated yields are shown. [a]Pyrimidinium salt formation: Tf_2O (1.0 equiv.), aniline (1.0 equiv.), collidine (1.0 equiv.), EtOAc, −78 °C to room temperature. [b]Isolated yields of pyrimidinium salts. Crude vinamidinium salts were used in the recyclization step. [c]Isolated yields of vinamidinium salts either directly from pyrimidines or pyrimidinium salts. LiHMDS, lithium hexamethyldisilazide; LDA, lithium diisopropylamine; THF, tetrahydrofuran.

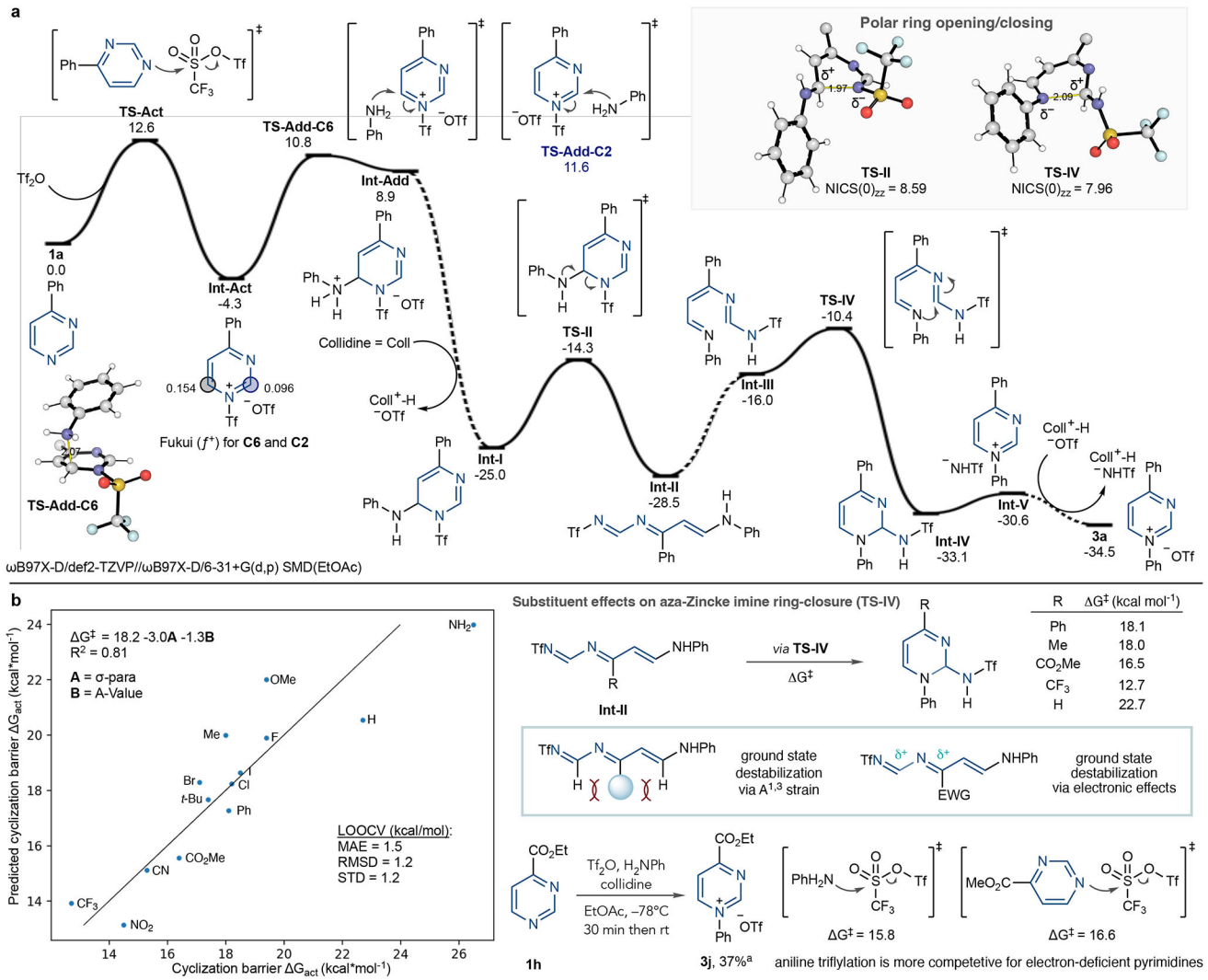

Fig. 5 |. Computational studies of pyrimidine ring-opening.

a, Quantum chemical computed reaction mechanism between pyrimidine **3a**, Tf_2O and aniline; relative Gibbs energies (195.15 K, 1 mol l^{-1}) in kcal mol^{-1}. **b**, Computational study of the steric and electronic effect of substituents on the cyclization of **Int-II** and *N*Tf-pyrimidinium salt formation. [a]^{1}H NMR yield reported. LOOCV, leave-one-out cross-validation; MAE, mean absolute error; r.m.s.d., root mean square deviation; s.d., standard deviation.